Polyductin undergoes notch-like processing and regulated release from primary cilia

Jun-ya Kaimori[1], Yasuyuki Nagasawa[2], Luis F. Menezes[1], Miguel A. Garcia-Gonzalez[1], Jie Deng[1], Enyu Imai[2], Luiz F. Onuchic[3], Lisa M. Guay-Woodford[4] and Gregory G. Germino[1,*]

[1]Division of Nephrology, Department of Medicine, Johns Hopkins University School of Medicine, Baltimore, MD, USA, [2]Department of Nephrology, Osaka University Graduate School of Medicine, Suita, Osaka, Japan, [3]Division of Nephrology, Department of Medicine, University of Sao Paulo, Sao Paulo, Brazil and [4]Division of Genetic and Translational Medicine, University of Alabama at Birmingham, Birmingham, AL, USA

Mutations at a single locus, *PKHD1*, are responsible for causing human autosomal recessive polycystic kidney disease (ARPKD). Recent studies suggest that the cystic disease might result from defects in planar cell polarity, but how the 4074 amino acid ciliary protein encoded by the longest open reading frame of this transcriptionally complex gene may regulate this process is unknown. Using novel *in vitro* expression systems, we show that the *PKHD1* gene product polyductin/fibrocystin undergoes a complicated pattern of Notch-like proteolytic processing. Cleavage at a probable proprotein convertase site produces a large extracellular domain that is tethered to the C-terminal stalk by disulfide bridges. This fragment is then shed from the primary cilium by activation of a member of the ADAM metalloproteinase disintegrins family, resulting in concomitant release of an intra-cellular C-terminal fragment via a γ-secretase-dependent process. The ectodomain of endogenous PD1 is similarly shed from the primary cilium upon activation of sheddases. This is the first known example of this process involving a protein of the primary cilium and suggests a novel mechanism whereby proteins that localize to this structure may function as bi-directional signaling molecules. Regulated release from the primary cilium into the lumen may be a mechanism to distribute signal to down-stream targets using flow.

INTRODUCTION

Autosomal recessive polycystic kidney disease (ARPKD) is a significant cause of pediatric morbidity and mortality, with an estimated incidence of one in 20 000 live births (1,2). The clinical spectrum is widely variable: ~30% of affected neonates die shortly after birth, whereas others survive into adulthood (3). In affected neonates, the kidneys are symmetrically enlarged and cysts appear as fusiform dilations of collecting ducts extending radially from the renal pelvis to the cortex (4). Congenital hepatic fibrosis, characterized by increased numbers of interlobular bile ducts and varying degrees of portal fibrosis, is an invariant finding.

Mutations of a single gene on chromosome 6, *PKHD1*, cause all typical forms of the disease in humans (5–8). The gene is ~470 kb in length and undergoes a complicated pattern of splicing to produce a complex set of transcripts (9,6).

A >12 kb mRNA that is composed of 67 exons encodes the longest open reading frame. The gene is most abundantly expressed in the kidney, though it is expressed in numerous other tissues at a low level. Almost 300 unique mutations have been described, and they have been identified in most of the 67 exons. Genotype–phenotype analyses suggest that the nature of the germline mutations plays an important role in determining clinical outcome. Missense substitutions are more commonly associated with non-lethal presentations, whereas chain-terminating mutations are more commonly associated with neonatal death (10–12). Individuals with two truncating changes universally do not survive beyond the neonatal period.

The expected gene product is a novel 4074 amino acid single-membrane spanning protein (fibrocystin/polyductin, referred to as PD1 in this article) that has a lengthy extracellular N-terminal domain made up of multiple TIG/

*To whom correspondence should be addressed at: Department of Medicine, Division of Nephrology, Ross 958, 720 Rutland Avenue, Baltimore, MD 20815, USA. Tel: +1 4106140089; Fax: +1 4106145129; Email: ggermino@jhmi.edu

IPT and PbH1 repeats and a short cytoplasmic C-terminus (6,13). It shares some features with members of the SEMA family of proteins but lacks several key domains of the latter. It is predicted to function either as a receptor, a ligand or possibly both, though there is no direct evidence for either. The gene's complex splicing profile, in fact, could lead to the generation of products with different domain combinations, which might be associated with distinct affinities or specificities for target ligands/receptors.

Several lines of evidence link PD1 to the function of the primary cilia. A comparative genomic approach identified a distantly related *PKHD1*-like gene product as a likely component of the flagella–basal body proteome of the single-cell organism, chlamydomonas (14). Masyuk *et al.* (15) reported that the primary cilia of biliary epithelia of pck rats were stunted and have gross morphological abnormalities. Finally, multiple groups have localized PD1 to the primary cilia/basal body (13,15–17). The protein may also be present at other domains within the apical membrane and within the cytoplasm.

Despite its clear link to disease, little is known about the function of PD1. It is presumed to have essential developmental functions, given the pre-natal and peri-natal disease manifestations that result when it is mutated. Studies of the Pck rat suggest that the protein may play a role in helping to establish planar orientation of developing renal tubules (18). In normal fetal tubules, the mitotic spindle of dividing cells is oriented along the long axis of elongating renal tubules. In the fetal tubules of pre-cystic kidneys of Pck rats, however, mitotic orientations are significantly distorted. How PD1 might help to regulate this process was not determined.

PKHD1 also is expressed in adult tissues, suggesting probable post-developmental functions. In the only published study of the gene's function, Mai *et al.* (19) used short hairpin RNA (shRNA) inhibition to reduce expression of the murine *Pkhd1* ortholog in IMCD cells and found that *Pkhd1*-silenced cells developed abnormalities in cell–cell contact, actin cytoskeleton organization, cell–ECM interactions, cell proliferation and apoptosis. Their data suggested that these effects might be mediated by dysregulation of extracellular-regulated kinase and focal adhesion kinase signaling. The mechanisms underlying these effects were not defined, however.

In this report, we describe a new *PKHD1 in vitro* expression system whose features include regulated expression of constructs with N-terminal and C-terminal epitope tags in HEK 293 and MDCK cell lines and show that PD1 undergoes a series of complicated post-translational modifications similar to those described for Notch. We demonstrate that the ectodomain of recombinant PD1 undergoes regulated shedding from the primary cilia and that endogenous PD1 shares similar properties. We propose a novel model by which the shed PD1 ectodomain might help to regulate planar orientation.

RESULTS

Full-length PD1 is a >500 kDa protein that undergoes a complicated pattern of proteolytic processing

We used high-fidelity polymerases to amplify three overlapping fragments that span the 67 exons that encode the longest ORF for human *PKHD1* from a human kidney cDNA library. Although many of the clones contained a variable assortment of exons, a set was found to include the full coding sequence as previously reported (6). Several point mutations were identified by double-strand sequencing and corrected by site-directed mutagenesis. The fragments were then assembled into a single full-length cDNA using unique restriction enzyme sites common to the overlapping segments (Fig. 1A). The final product was again sequenced to confirm that all errors had been corrected and cloned into a mammalian expression vector (pCI). FLAG or EGFP tags were added to the N-terminus and 7XMyc tag was added to the C-terminus to allow better detection (Fig. 1B). The expression level of this construct was too low to use practically, so we added an additional beta-globin intronic sequence between the promoter and *PKHD1* cDNA sequence to enhance protein expression. We verified expression of the full-length PD1 by transient expression in HEK 293 cells and determined that it was >500 kDa (Fig. 1C).

In immunoprecipitating the full-length product with anti-Myc beads and immunoblotting with anti-Myc antibodies, we identified a set of additional, smaller products present in cells expressing recombinant PD1 but not in control cells (Fig. 1D). These smaller products were thought likely to be proteolytic, C-terminal products derived from the full-length construct. We confirmed this to be the case using two additional *PKHD1* constructs, ΔE-PD1 and PICD, which lack either just the extracellular domain or everything but the intra-cytoplasmic domain (Fig. 1B). These constructs yielded both their expected full-length sizes and a similar pattern of shorter fragments <50 kDa (Fig. 1D).

PD1 is cleaved to produce a PD1 extracellular domain and a PD1 transmembrane fragment which are tethered together by disulfide bonds

To better determine the properties of PD1, we established a set of HEK 293 (human embryonic kidney) and MDCK II (Madin–Darby canine kidney) cell lines with stable, inducible expression of epitope-tagged recombinant full-length *PKHD1*. In characterizing the cell lines, we identified another PD1-derived, C-terminal product of ~85 kDa that appeared ~48 h after induction of *PKHD1* expression (Fig. 2A). Using biotinylation cell-surface labeling studies, we determined that it was located on the cell surface, as was the full-length molecule. These data prompted us to examine the extracellular PD1 amino acid sequence for potential proteolytic sites. Using the Prop1.0 server (www.cbs.dtu.uk/services/ProP), we identified several potential proprotein convertase (PC) cleavage sites that met the consensus sequence ([R/K]-Xn-[R/K] $n = 0,2,4$ or 6) (20) in the human polyductin extracellular domain (PECD). However, the site at position 3617–3620 was the most highly conserved in multiple species (human AAM93492, mouse AAN05018 and dog XP_532169), with the highest prediction score in each (0.803 human, 0.705 mouse, 0.872 canine) (Fig. 2B).

The PC family in mammals includes at least eight members, with furin being its most thoroughly investigated member. It is not likely, however, to be the PC responsible for cleavage of
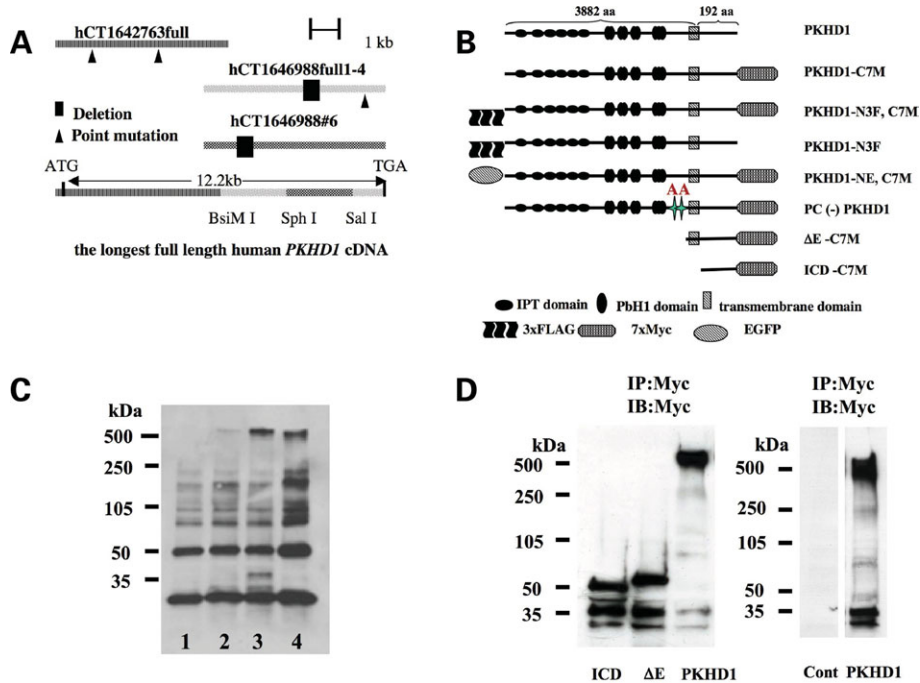
Figure 1. Expression system for recombinant human PD1. (**A**) Three overlapping fragments (hCT1642763full, hCT1646988full 1–4 and hCT1646988#6) were synthesized by RT–PCR using human kidney RNA as template. Bi-directional sequencing had identified several single base pair differences and small deletions compared with the published sequence (6,7), which were corrected by site-directed mutagenesis and selective use of sub-fragments. The fragments were assembled to produce a full-length cDNA for the longest predicted *PKHD1* ORF using the restriction sites indicated. (**B**) Schematic representation of the full-length (PKHD1-) and truncated (ΔE-, ICD-) PD1 proteins with epitope tags at either their N- [3× FLAG (-N3F), EGFP (-NE)] or C- [7x-Myc (-C7M)] termini that are described in this report. All N-terminal tags were placed after the signal peptide sequence. The sizes of the cytoplasmic C-terminal and the extracellular/transmembrane fragments are expressed as the number of amino acid residues. (**C**) Full-length recombinant PD1 is >500 kDa in size. Whole cell lysates were prepared from cells transiently transfected with empty vector (pCI) (lane 1), PKHD1-C7TM with a single intron (lane 2), PKHD1-C7TM with a double intron (lane 3) or Myc-PKD1 (lane 4) and then incubated with anti-Myc antibodies coupled to agarose beads. The affinity-purified products were separated by 4–15% PAGE, immunoblotted and probed with anti-Myc antibodies. A faint band >500 kDa that is approximately equal in size to polycystin-1 (lane 4) is seen in lane 2 and in much greater abundance in lane 3, but is not present in the negative control (lane 1). Two smaller novel bands of ~37 and 30 kDa also are seen in lane 3. (**D**) The C-terminus of PD1 undergoes a complicated pattern of proteolytic processing. Left panel: ICD-C7M (ICD), ΔE-C7M (ΔE) and PKHD1-C7M (PKHD1) were transiently expressed in HEK 293 cells, affinity purified using anti-Myc beads and then immunoprobed using anti-Myc. Two smaller fragments of ~37 and 30 kDa were present in each of the three samples in addition to predicted full-length products (~50, 65 and >500 kDa, respectively). The Myc epitope tag is noted to increase the apparent molecular weight of ICD-C7M and ΔE-C7M by ~25 kDa. Right panel: Control experiments demonstrating specificity of Myc antibodies. Lysates were prepared from HEK 293 cells transfected with either empty vector (Cont) or PKHD1, subject to affinity enrichment and then immunoprobed using anti-Myc beads and antibodies, respectively. *PKHD1*-expressing cells yielded the expected pattern, whereas no bands were detected in the control sample.

PD1, given its substrate specificity preferences. Furin preferentially recognizes sites that contain the sequence motif RX[R/K]R (21) and does not accept lysine (K) residues at the subsequent two positions (22). The PD1 amino acid sequence does not satisfy these requirements. We also experimentally excluded furin as the responsible PC by showing that known furin inhibitors, α1-antitrypsin Portland and decanoyl-RVKR-chloromethylketone, could not inhibit PD1 cleavage (data not shown).

If the putative PC site was active, we would then expect an N-terminal fragment (PECD) to remain tethered to the remainder of the molecule [PD1 transmembrane fragment (PTM)] (Fig. 2B). Consistent with this model, we found two cysteines immediately C-terminal to the putative PC sequence and a matching pair equally spaced apart in the N-terminal sequence (Fig. 2B). Like the PC site itself, the cysteine pairs also are present in other species. Notably, one of the cysteines was found mutated to arginine and another was mutated to tyrosine in patients with ARPKD (Fig. 2B) (23). To confirm our

prediction, we immunopurified PD1 using anti-Myc beads and immunoblotted using either anti-Myc antibodies or antibody 5509 raised against a peptide derived from the human PD1 C-terminus. Both antisera recognized identical full-length and 85 kDa PTM fragments (Fig. 2C). Probing the same blot with C2, an antibody raised against a polypeptide derived from the N-terminal domain of PD1, we saw both the full-length and PECD molecules, as predicted (Fig. 2C). In contrast, the 85 kDa PTM fragment was not detected when the PC site of PD1 was mutagenized by replacing K3167 and R3618 with two alanines (Fig. 1B and 2D). These data suggest that the PC site is responsible for the observed cleavage.

Our model also predicts that PECD should be tethered to PTM by disulfide bonds. We found this to be the case, as shown in Figure 2E. We detected PTM in cell lysates of cells expressing polyductin, which had been treated with β-mercaptoethanol, but not in lysates not treated with this reducing agent.
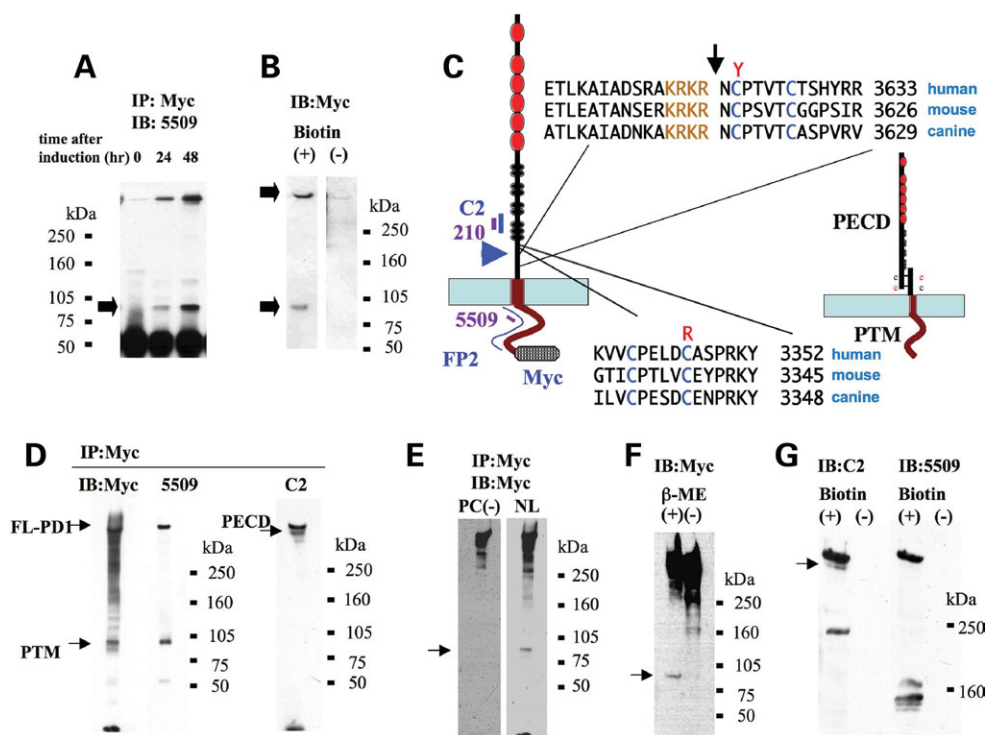
Figure 2. The PECD is cleaved at a probable PC site and is tethered to the C-terminal stalk. (**A**) Total cell lysates prepared from HEK 293 cells with stable, inducible expression of PKHD1-N3F, C7M at 0, 24 and 48 h post-induction were incubated with anti-Myc agarose beads and immunoprobed with 5509. Both the full-length product and a shorter 85 kDa product (arrow) were detected 24 h post-induction. (**B**) Cell-surface biotinylation assay of *PKHD1*-expressing cells. Total cell lysates of the same cell line used in (A) were prepared from cells either incubated with (+) or without (−) biotin prior to cell harvesting, subject to affinity purification using streptavidin-conjugated agarose beads, immunoblotted and then probed with anti-Myc antibodies. Both the full-length and 85 kDa products were detected in the biotinylated sample (arrows), with minimal background in the non-biotinylated negative control. (**C**) PD1 has a probable PC cleavage site in its extracellular domain. On the left is a schematic representation of PD1 and the relative position of epitopes recognized by antibodies used in this study (in blue, purple). Immediately adjacent to it is the sequence of a putative PC sequence that is highly conserved in vertebrates (light brown). The arrow identifies the position of the predicted cleavage site in the sequence and the blue arrowhead identifies the relative location of the site with respect to the protein's overall structure. The sequences at the bottom are of the domain likely responsible for tethering the N-terminal cleavage fragment to the C-terminal stalk post-cleavage. The cysteines thought likely to mediate this interaction are colored in blue, and disease-associated missense changes affecting these residues (Y, R) are shown in red. On the far right is a cartoon illustrating the predicted final product that results from PC cleavage, with the extracellular N-terminus (PECD) tethered to the C-terminal stalk (PTM). (**D**) Immunoprecipitation of PD1 from MDCK cell lines with stable, inducible expression of PD1 using Myc-coupled agarose beads and immunoprobed with the antibodies indicated. Antibodies that recognize epitopes in PTM (Myc, 5509) detect both the full-length and 85 kDa products, whereas the one that recognizes an epitope in the PECD detects both the full-length and tethered PECD products. The same blot was used for immunoprobing with Myc and C2. (**E**) The putative PC cleavage sequence is responsible for the observed cleavage. We generated a set of MDCK cell lines with stable, inducible expression of a mutant form of PD1 in which the PC sequence was mutagenized from KRKR to AAKR [PC(−)]. Total cell lysates were prepared 48 h post-induction from PC(−) cells expressing mutant PD1 and MDCK cells expressing wild-type PD1 (NL), incubated with anti-Myc beads and then immunoblotted with anti-Myc antibodies. PTM is not present in lysates prepared from the PC(−)-expressing cells (arrow). Because expression levels of mutant PD1 are considerably lower in the PC(−) cell lines than are levels of normal PD1 in NL cell lines, we adjusted exposure times to yield images of approximately equal intensity for this figure. (**F**) PECD is tethered to PTM by disulfide bonds. Total cell lysate was prepared from MDCK cells induced to express PKHD1-N3F,C7M and then either treated (+) or not treated (−) with β-mercaptoethanol prior to PAGE and immunoblotting. The 85 kDa PTM fragment is detected by anti-Myc antibodies only under reducing conditions (arrow). (**G**) PECD is present on the cell surface. Same experimental design as in (A), except the streptavidin-affinity purified products were probed with C2. The blot was then stripped and re-probed with 5509.

We note that the apparent size of the PTM is larger than predicted, based on its primary sequence. This is due, in part, to the 7-Myc tag that was added to the C-terminus. The remainder is due to probable conformation effects that the 7-Myc tag exert on the protein's migration in SDS–PAGE gels. This is clearly illustrated by the apparent sizes of the similarly tagged shorter *PKHD1* variants ICD-C7M and ΔE-C7M (Fig. 1D), which appear ~25 kDa larger than their primary sequences would predict. These data, together with the results of the PC site mutagenesis study, strongly suggest that the 85 kDa band is the expected PECD product.

The ectodomain of PD1 undergoes regulated and constitutive shedding

Given that many other molecules that undergo PC processing also undergo regulated ectodomain shedding, we tested for this property for PD1. We transiently expressed two different epitope-tagged *PKHD1* constructs in HEK cells, used FLAG beads to affinity purify secreted product shed into the media and then immunoprobed the western blot using anti-FLAG antibodies. As shown in Fig. 3A, a similar large product slightly smaller than full-length PD1 was detected in the media in cells expressing each construct. We next examined
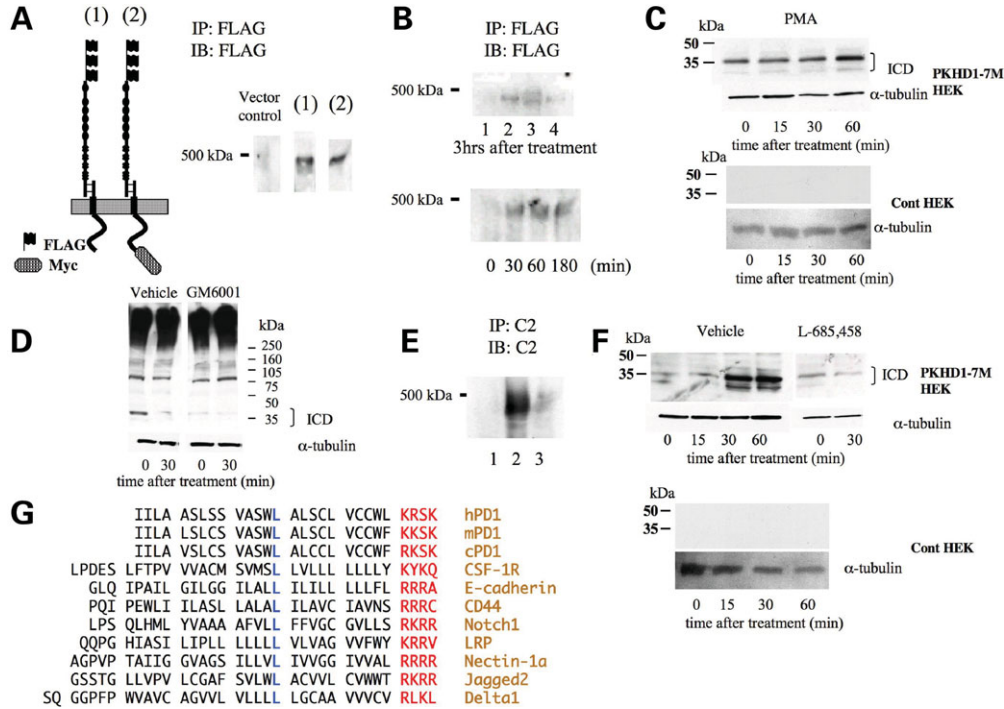
Figure 3. PD1 undergoes both constitutive and regulated ectodomain. (**A**) Constitutive ectodomain shedding of PD1. N-terminally FLAG-tagged PKHD1 either with (2, PKHD1-N3F,C7M) or without (1, PKHD1-N3F) a C-terminal Myc epitope was transiently expressed in HEK 293 cells. After 48 h of induction, tissue culture media was collected and the PD1 ectodomain was immunopurified from the media using FLAG beads. A band slightly lower than 500 kDa was detected in the media of cells expressing either construct. (**B**) Stimulated ectodomain shedding of PD1. Top: HEK 293 cells with stable, inducible expression of *PKHD1* were induced to express PD1 and then placed in fresh tissue culture medium containing various known activators of metalloproteases. The media were collected at the end of 3 h and then tested for the presence of PECD. Lane 1: negative control; lane 2: pervanadate (100 μM); lane 3: 20% FBS; lane 4: calcium ionophore (1 μM). Bottom: Time course of regulated release of PECD. The same *PKHD1+* cell was treated with PMA (100 ng/ml), another known activator of metallo-proteases, for the times indicated and then the medium collected at each timepoint was tested for PECD. (**C**) PD1 undergoes stimulated intra-cellular domain (ICD) cleavage concomitant with its ectodomain shedding. Top: Same cell line used in (B) was treated with PMA (100 ng/ml) for the times indicated and then cell lysates were immunoblotted and probed with anti-Myc. A constitutive 37 kDa product increases in abundance upon PMA stimulation. The same blot was probed for α-tubulin to show that approximately equal quantities of lysate were loaded in each lane. Bottom: A vector-transfected control HEK 293 cell line treated in an identical manner as the *PKHKD1+* cell line and probed with anti-Myc (top) and anti-tubulin (bottom). (**D**) Inhibitors of metalloproteases block release of ICD. On the left, lysates of same *PKHD1+* cell line used in (B) and (C), which had been treated for the indicated times with a calcium ionophore and diluent (DMSO, 'vehicle'), immunoblotted and probed with anti-Myc. On the right, the identical experimental design except the broad metalloprotease inhibitor GM6001 was added to the diluent and calcium ionophore at a final concentration of 50 μM for the indicated times. The blots were then re-probed for α-tubulin to confirm equal loading. (**E**) Inhibitors of metalloproteases block release of PECD. An MDCK cell line with inducible expression of PKHD1-C7M was treated with a calcium ionophore for 30 min either with (lane 3) or without (lane 2) GM6001 (150 μM final) and then the medium was tested for PECD by immunoprecipitating and immunoblotting with C2. Lane 1 is media from the same cell line, without treatment with a calcium ionophore. (**F**) Top: Same experimental design used in (D), except the γ-secretase inhibitor L-685,458 was substituted for GM6001 at a final concentration of 5 μM. Bottom: Lysates of a HEK 293 vector control cell line treated in an identical manner with a calcium ionophore and a vehicle, immunoprobed with anti-Myc and anti-tubulin antibodies. (**G**) Alignment of transmembrane domains of various known γ-secretase substrates. The stop-transfer signal is highlighted in blue and a highly conserved leucine that is positioned 11 residues away is in red. The names of the proteins are listed to the far right in light brown.

whether this process is regulated by activation of ADAM metalloproteinase disintegrins, as has been reported for other molecules that undergo ectodomain shedding (24). We treated the cells with known activators of ADAM sheddases including pervanadate, the calcium ionophore A23187, 20%FBS and phorbol 12-myristate 13-acetate (PMA) and found that all induced PD1 ectodomain shedding (Fig. 3B).

PD1 undergoes regulated intra-membrane proteolysis with release of intra-cytoplasmic products (PICD)

A number of proteins that undergo regulated ectodomain shedding have a concomitant cleavage and release of intra-cellular, cytoplasmic fragments. We tested PD1 for this property in cells treated with two of the compounds found to activate

PD1 ectodomain shedding. Using the calcium ionophore A23187 and PMA, we saw a time-dependent increase in cytoplasmic products in response to these treatments (Fig. 3C). We also found that a broad metalloprotease inhibitor, GM6001, inhibited this process and reduced release of ICD and shedding of PECD (Fig. 3D and E). In many other proteins, the regulated cleavage of the intra-cellular domain is mediated by γ-secretase. Although there is no specific consensus sequence indicating the likely location of a γ-secretase-sensitive site, an alignment of the transmembrane domain sequence of molecules with known γ-secretase substrates reveals a well-conserved leucine 11 residues from the stop-transfer signal that also is present in PD1 (25) (Fig. 3G). We therefore tested whether γ-secretase played any role in the proteolysis of PD1 using the inhibitor L-685,458. Although we found

that it could not inhibit the constitutive cleavage of intra-cellular domain of PD1 (data not shown), it did inhibit the release of C-terminal products that are produced in response to treatment with an inducer of ectodomain shedding (calcium ionophore, Fig. 3F). These data indicate that the C-terminus of PD1 undergoes both constitutive and regulated cleavage, the latter mediated by γ-secretase.

PECD is shed from primary cilia

Endogenous PD1 has been previously localized to the primary cilium. We therefore determined whether recombinant PD1 trafficked to the same location in MDCK II cells grown up to 14 days post-confluence on Transwell filters. We added epitope tags to either the C-terminus (7 × Myc, PKHD1-C7M) or both the N- and C-termini (EGFP and 7 × Myc, PKHD1-NE,C7M), so that we could distinguish between signals from recombinant and endogenous proteins and use these constructs to generate stable cell lines with inducible expression (Fig. 1B). Flp-In-MDCKII cells transfected with empty vector and cultured in an identical manner to the *PKHD1+* cells were used as a negative control. Although we had sought to track expression using EGFP fluorescence, signal intensity was too low to be used practically. Therefore, co-localization studies were performed using antibodies that recognize EGFP or Myc with antibodies to acetylated tubulin, a marker for primary cilium. As shown in Figure 4, acetylated tubulin co-localized with PD1 in the *PKHD1+* cell lines, though PD1 had a speckled distribution pattern as has been previously described for other ciliary proteins that undergo intra-flagellar trafficking (26,27) (Supplementary Material, Movie S1). We next tested how activators of ecto-domain shedding affected the sub-cellular distribution pattern of PD1. Cells were cultured to post-confluence on Transwells, treated with a calcium ionophore and then stained with anti-EGFP and anti-Myc antibodies at various times post-treatment (Fig. 5). Within 30 min of activation, the majority of cilia lacked staining for both EGFP and C-terminal Myc tag, but remained positive for acetylated tubulin. Cilia also retained staining for Vangl2, another ciliary protein, excluding non-specific effects of our interventions on intra-flagellar transport as a trivial explanation for our findings (Supplementary Material, Fig. S1) (28).

PD1 C-terminus localizes to the nucleus

By analogy to Notch, we predicted that the C-terminal fragment of PD1 would translocate to the nucleus once released from the rest of the molecule by γ-secretase. However, only a low amount of nuclear staining was detected using antisera for the C-terminal tag of PD1 in cells expressing the full-length protein at baseline, and its intensity did not appreciably increase in response to activation (Fig. 5). Similar problems had been encountered with Notch and had been attributed to the relatively low abundance and short half-life of the clea-vage products (29,30). We therefore generated MDCK cell lines with inducible expression of an epitope-tagged cyto-plasmic C-terminus of PD1 (ICD-C7M, Fig. 1) and deter-mined where it localized within the cell. Nuclear staining was readily apparent upon induction of expression (Fig. 6),

indicating that the C-terminus is capable of translocating to the nucleus under suitable conditions.

Endogenous PD1 protein is shed from the primary cilia

In a final set of experiments, we sought to determine whether endogenous PD1 was subject to the same processing as the recombinant molecule. We selected IMCD cells, an SV-40 immortalized cell line derived from mouse inner medullary collecting duct epithelium (31), for these studies since they have previously been reported to express PD1 (16,19). We first confirmed expression of PD1 in IMCD cells by reciprocal immunoprecipitation/immunoblot studies using FP-2, C2, 5509 and 210 antibodies. All of the antibodies recognized an identically sized, high molecular weight protein similar in size to the full-length recombinant protein; however, we were unable to identify PTM unambiguously by this technique since its predicted size is similar to that of IgG (data not shown). We attempted to circumvent this problem by examin-ing the pattern of PD1 expression in whole cell lysates, but were unsuccessful because of its very low level of expression. We therefore investigated the effects of sheddases on PD1 expression on a cellular level using confocal microscopy. Using antibodies that recognize epitopes in both the extra-cellular and intra-cellular portions of PD1, we found that PD1 localized to the primary cilia of IMCD cells cultured to post-confluence on Transwells, but disappeared from this structure upon stimulation with a calcium ionophore (Fig. 7A; Supplementary Material, Movie S2). Moreover, we found that prior treatment with the broad metalloprotease inhibitor GM6001 prevented shedding of PD1, whereas treat-ment with vehicle alone did not (Fig. 7B). These data strongly suggest that endogenous PD1 has the same key properties exhibited by the recombinant molecule.

DISCUSSION

The ARPKD gene, *PKHD1*, is predicted to encode a novel protein of 4074 amino acids with a single TM and multiple IPT and PbH1 domains in its extracellular portion, but whose function is largely unknown. *PKHD1* undergoes a com-plicated pattern of splicing and therefore may encode a variety of additional gene products. These facts make investigation of its gene product, PD1, particularly difficult. Given the many challenges that this gene's complexity posed, we developed a set of novel *in vitro* expression systems to study its function. By using a recombinant system with epitope tags, we could unambiguously track PD1 and then use this information to guide our study of the endogenous protein. The fact that we could show that the endogenous protein shares many of the properties defined for the recombinant molecule validates our system.

Using these tools, we discovered that PD1 is a plasma membrane-associated protein that undergoes a complicated pattern of proteolytic processing, producing multiple smaller products. We determined that some of the proteolytic reactions were regulated, whereas others appeared constitutive under the conditions used. We found a likely PC site in the extracellular domain of PD1 that appears responsible for producing a large,
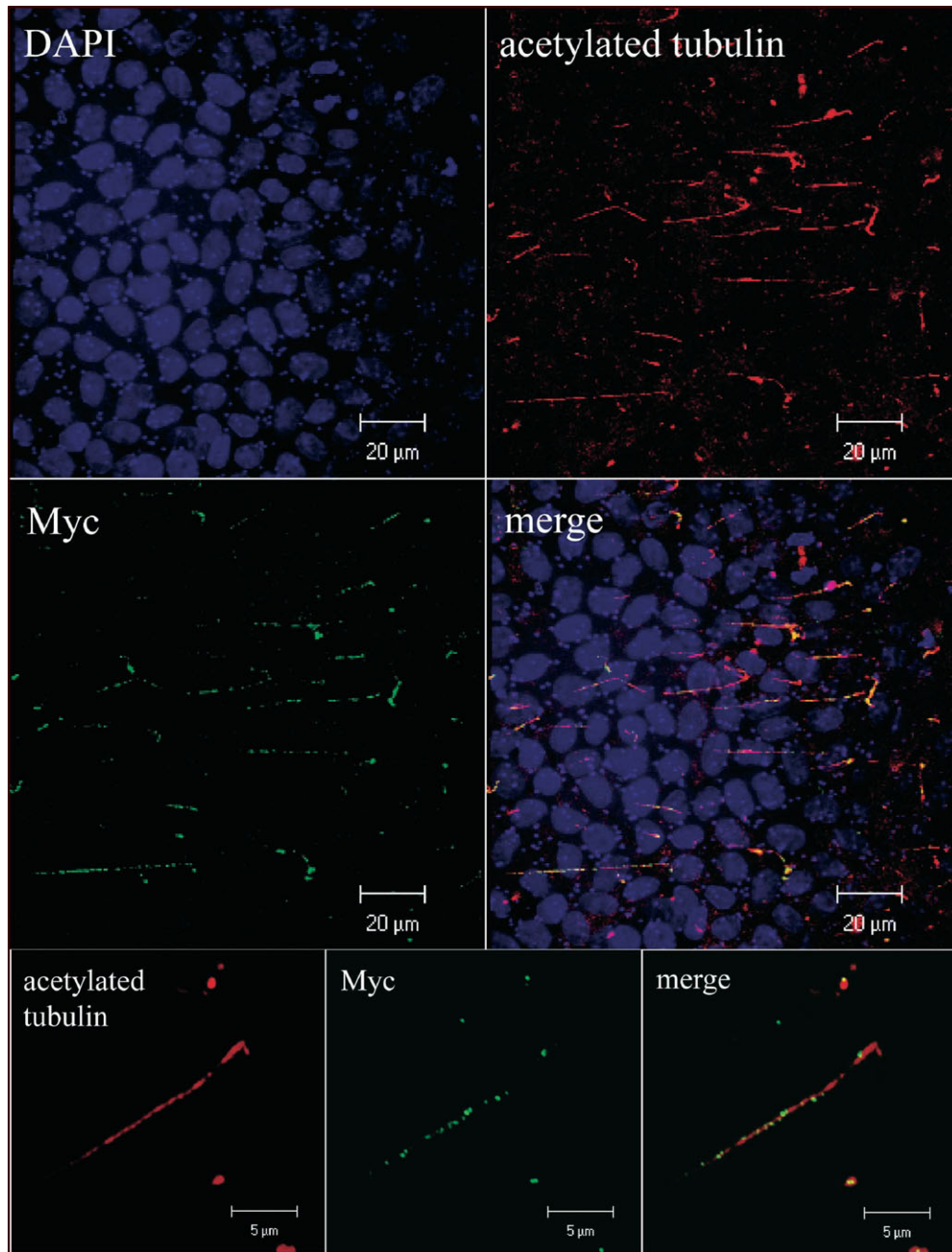
Figure 4. Recombinant PD1 localizes to the primary cilium. Three-dimensional reconstruction of confocal images projected in the $X-Y$ plane of MDCK cells expressing PKHD1-C7M cultured for 14 days post-confluence on Transwell filters, fixed, permeabilized and then immunostained for acetylated tubulin and Myc. The top four panels were imaged at $100\times$ and the bottom three insets were viewed at $400\times$ (Supplementary Material, Movie S1).

tethered N-terminal fragment present on the cell surface. Our studies suggest that a member of the ADAM metalloproteinase disintegrins family mediates shedding of this fragment. We also found that cleavage at this extracellular site is required for the concomitant regulated release of an intra-cellular C-terminal fragment, the latter step apparently a γ-secretase-dependent process. We used confocal analysis to show that PD1 that is localized to the primary cilium undergoes regulated shedding and intra-membrane proteolysis (RIP).

Finally, we confirmed that endogenous mouse PD1 has many of the same properties.

Since submission of our manuscript, Hiesberger *et al.* (32) have described complementary studies that support our findings. They expressed an epitope-tagged form of the human full-length *PKHD1* cDNA in IMCD and HEK cells and similarly detected a series of proteolytic products, including a C-terminal product that localized to the nucleus. They also found that release of the intra-cellular product was both
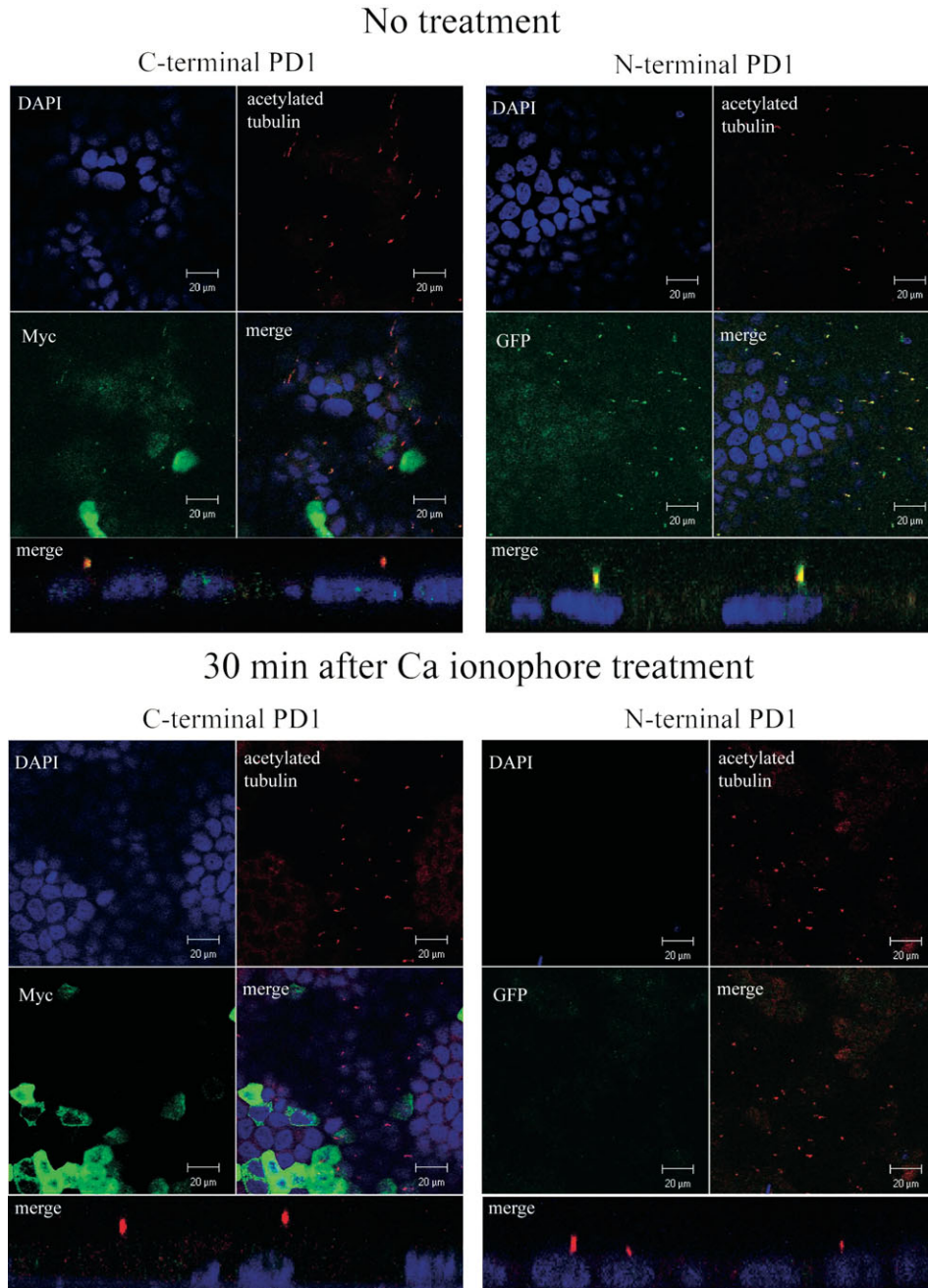
Figure 5. Recombinant PD1 is shed from the primary cilium. Confocal images of MDCK cells with stable, inducible expression of PKHD1-NE,C7M, which were cultured for 7 days post-confluence on Transwell filters and either left untreated (top) or treated with a calcium ionophore to induce ectodomain shedding for 30 min prior to preparation for imaging. 'C-terminal PD1' identifies panels where specimens were co-stained with DAPI (blue), anti-Myc (green) and anti-acetylated tubulin (red). 'N-terminal PD1' identifies panels where specimens were similarly co-stained, except anti-EGFP (green) was used in place of anti-Myc to detect PD1. The reduced DAPI signal apparent in the bottom right set of panels is because the focal plane is above that of the nuclei in this image. All images were captured at $100\times$. The four panel images are $X-Y$ sections, whereas the single merge image below each the four panel sets is a representative Z section.

constitutive and regulated by calcium and speculated that the process occurred in conjunction with ectodomain shedding. A putative nuclear localization sequence was identified in the C-terminus by deletion mapping. One difference between our findings and theirs is with respect to the nuclear localization pattern of our respective products. Hiesberger *et al.* described a nucleolar pattern, whereas we found a more

punctate pattern consistent with localization to nuclear bodies or splicing speckles. This discrepancy may be due to differences in the epitope tags, cell lines or other unidentified factors. Further study will be required to resolve this issue.

The post-translational pattern of proteolytic processing of PD1 is very similar to what has been previously described for the key developmental protein, Notch (33,34). Notch is
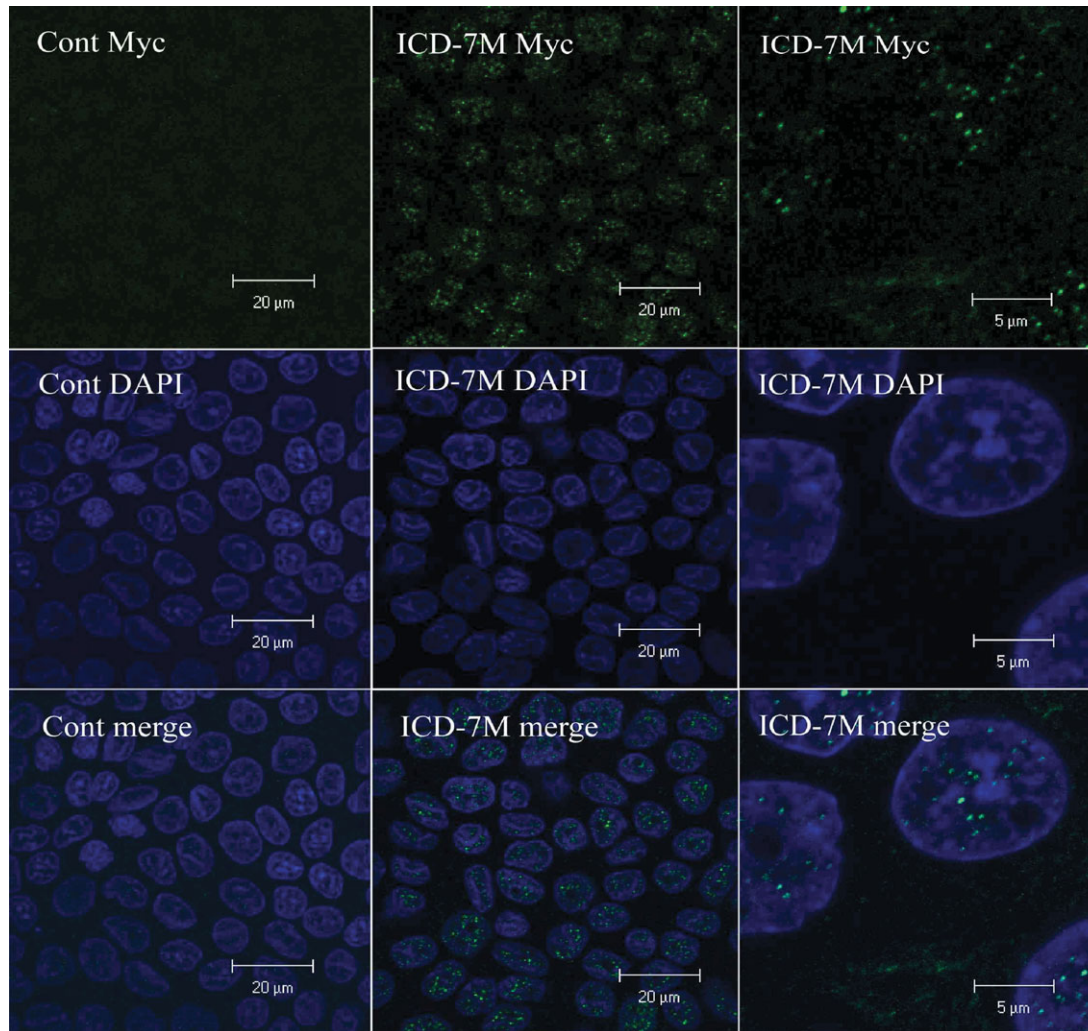
Figure 6. The PD1 C-terminus localizes to the nucleus. Confocal images of MDCK cells with either stable, inducible expression of empty vector (left, Cont Myc) or ICD-C7M (middle), which were cultured for 7 days post-confluence on Transwell filters and stained with an anti-Myc antibody (top, green) and DAPI (middle, blue). The images at the bottom are the merged images of the upper and middle panels. The images on far left were captured at $100\times$ and those on the right were taken at $400\times$.

synthesized as a single TM-spanning protein whose large extracellular domain is first cleaved by furin and then is tethered to the remainder of the protein. The mature receptor is expressed on the cell surface and its ectodomain is shed in response to binding of its ligand (Jagged and other ligands). Ligand binding also results in regulated RIP and release of a cytoplasmic C-terminus that enters the nucleus and switches a DNA-bound co-repressor complex into one that is activating. There also is evidence that the shed Notch/ligand complex may have additional functional activity, suggesting that Notch has bi-directional signaling. We hypothesize that PD1 may have similar properties. The shed ectodomain may function as a ligand for other cellular receptors, whereas its RIP product may have direct signaling functions.

We also note that Notch and PD1 have a number of dissimilar features that likely reflect differences in their underlying function. In the case of Notch, the receptor–ligand interaction occurs between adjacent cells and functions to determine cell fate. In the case of PD1, we cannot unambiguously localize the protein to the site of cell–cell interactions in the cell types examined. Instead, we have shown that it traffics to the primary cilium from where it undergoes regulated shedding. This result has a number of important implications. First, it may mean that ectodomain shedding and RIP for PD1 are not ligand-mediated but instead regulated by other processes that locally activate ADAM sheddases. Such a mechanism has been described for transactivation of the EGF receptor by G-protein-coupled receptors (GPCR). Ligand binding to GPCR activates an ADAM sheddase, which then results in release of EGF ligand (35). In the case of PD1, activation of other ciliary receptors or flow-mediated changes in calcium flux may mediate this process. Alternatively, PD1 may function like Notch as a receptor, but its ligand is either a secreted molecule present in the lumen or a factor also present on the surface of the primary cilium. This observation, coupled to the fact that the ectodomain is shed into the lumen and thus
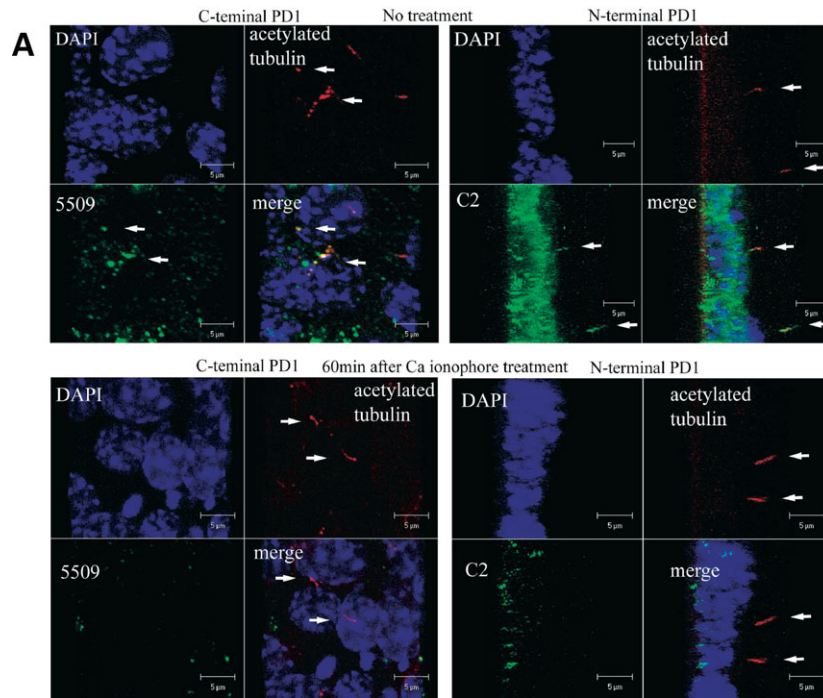
Figure 7. Endogenous PD1 undergoes regulated ectodomain shedding. (**A**) Endogenous PD1 is shed from the primary cilium. Three-dimensional re-construction of confocal images of IMCD cells cultured for 7 days post-confluence on Transwell filters and either left untreated (top) or treated with a calcium ionophore to induce ectodomain shedding for 60 min prior to preparation for imaging. 'C-terminal PD1' refers to a set of specimens stained for acetylated tubulin to identify the primary cilia and for the C-terminus of PD1 using antiserum 5509. The projected $X–Y$ plane is presented. 'N-terminal PD1' refers to a similar set of specimens stained with antibodies for acetylated tubulin and the N-terminus of PD1 using antiserum C2 and presented as a projection of the Z-axis. Arrows identify representative primary cilia. The data clearly show that PD1 is shed from the primary cilium under these experimental conditions. All images were captured at $400\times$ (Supplementary Material, Movie S2). (**B**) The metalloprotease inhibitor GM6001 inhibits shedding of endogenous PD1 from the primary cilia. Similar experimental design as the one used for (A) except the metalloprotease inhibitor GM6001 was added to the medium for 60 min prior to treatment with a calcium ionophore to induce shedding. Cells were treated with a calcium ionophore and either GM6001 or vehicle (DMSO) for 60 min prior to preparation for imaging. Specimens were stained for acetylated tubulin to identify the primary cilia and for either the C-terminus of PD1 using antiserum 5509 (top) or the N-terminus of PD1 using antiserum C2 (bottom). The projected $X–Y$ plane is presented on top and a projection of the Z-axis is shown below. All images were captured at $100\times$.

potentially projected beyond adjacent cell boundaries, suggests important functional differences between Notch and PD1.

We presently are unable to determine whether the PD1 intra-cellular cleavage products have a fate similar to that of Notch. Under standard conditions, we detect C-terminal signal in the nucleus by confocal analysis, but we have not yet been able to unequivocally demonstrate an increase in nuclear signal after induction of ectodomain shedding and RIP. This is not necessarily surprising since the products may be short-lived and of low abundance. Similar problems had been encountered with Notch (29,30). In the absence of a known set of transcriptional targets or nuclear co-factors, it may be difficult to demonstrate a nuclear function for PD1's terminal cleavage products. Further study will be required to resolve this issue.

As noted, there was an additional set of C-terminal products and a high molecular weight N-terminal product that were constitutively present in the cell cytoplasm and tissue culture medium, respectively. We presently are unable to determine whether these are the result of low-level activation of regulated cleavage or the result of different processes. We also do not know where in the cell the precursor form of PD1 is

localized at the time of cleavage or whether endogenous PD1 has this same property. Addressing the last question will be a considerable challenge, given the relatively low level of expression of PD1 in IMCD cells.

The observation that the extracellular domain is shed from the primary cilium prompts speculation as to what it may do. It is possible that the domain primarily serves as a receptor and that the shed fragment has no function post-release from the cell surface. A number of receptors are down-regulated by this mechanism. However, many ectodomains that are released from other integral membrane proteins have biologically significant properties, and we predict the same for PD1. One possibility is that the ectodomain functions in a paracrine fashion. In ductal and tubular epithelial cells that line lumens with flow, its release from primary cilia into the lumen may be a mechanism to distribute signal to down-stream or adjacent targets beyond the immediate point of cell–cell contact. One intriguing possibility is that flow-based delivery of the shed product may be a way of maintaining planar orientation with respect to the longitudinal axis (Fig. 8). In other cell types, cilia-based release may be a way to project signal beyond the immediate vicinity. This may serve as a means of coordinating the activity of a group of cells rather than that of just a
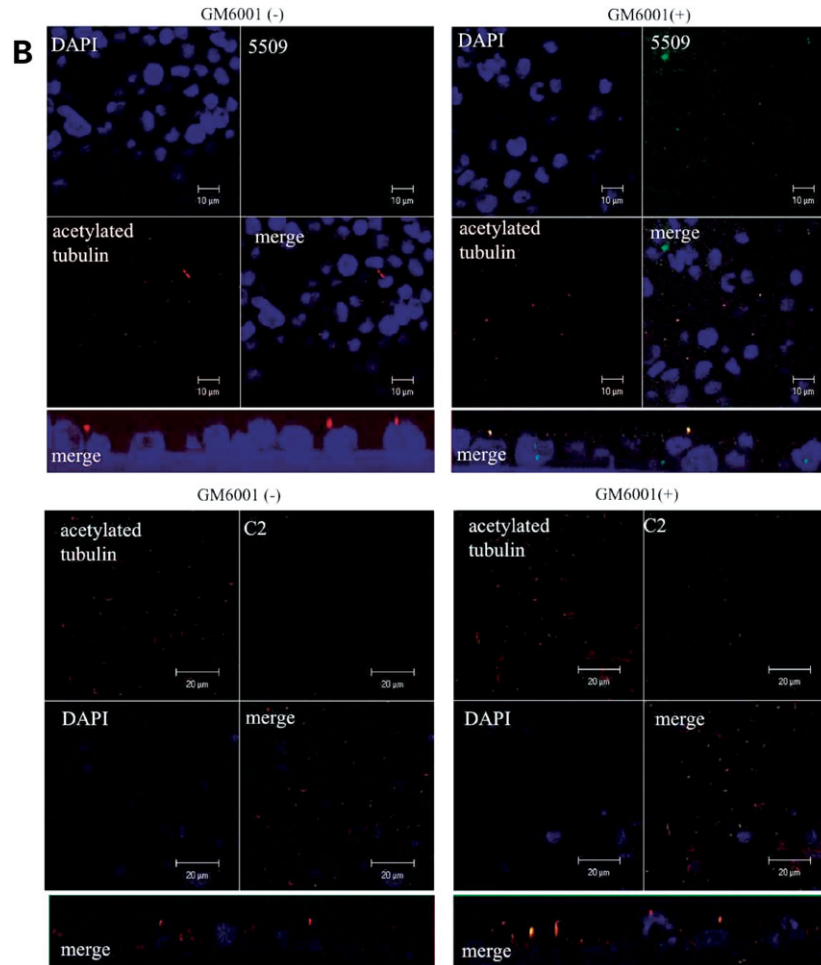
Figure 7. continued

single neighbor. This potentially could be an important way to coordinate the activity of cells to form tubular structures of defined diameter.

In conclusion, we have shown that PD1 undergoes Notch-like processing and regulated release of its ectodomain from primary cilia. This is the first known example of this process involving a protein of the primary cilium and suggests a novel mechanism whereby proteins that localize to this structure may function as bi-directional signaling molecules.

MATERIALS AND METHODS

Reagents

The following vendors were sources for the reagents used in this study: Roche Applied Science (Mannheim, Germany): monoclonal anti-Myc antibody and protease inhibitor cocktail; Sigma (Deisenhofen, Germany): mouse monoclonal anti-acetylated tubulin, polyclonal anti-FLAG antibody and M2 anti-FLAG beads, polyclonal anti-Myc beads, p3× FLAG-CMV10, A23187, PMA, sodium orthovanadate and hydrogen peroxide; Cell Signaling Technology (Danvers, MA, USA): rabbit anti-Myc antibody; Clontech (Palo Alto, CA, USA): monoclonal anti-Myc beads, rabbit anti-GFP antibody; Vector Laboratories (Burlingame, CA, USA): goat fluoresein-conjugated anti-rabbit IgG antibody and goat Texas Red conjugated anti-mouse IgG antibody; Molecular Probe (Eugene, OR, USA): Alexa-488 conjugated anti-fluoresein antibody; Pierce (Rockford, IL, USA): NHS-SS-biotin, streptavidin–agarose beads; Gibco/Invitrogen (Gaithersburg, MD, USA) DMEM, DMEM/F12 and heat-inactivated fetal bovine serum; Calbiochem (Darmstadt, Germany): GM6001 and L-685, 458; Invitrogen (Carlsbad, CA, USA): Flp-In T-Rex 293 cell line, pcDNA5/FRT/TO, pOG44, pFRT/lacZeo and pcDNA6/TR, pcDNA3.1, LipofectAMINE 2000; Promega (Madison, WI, USA): pCI vector; ATCC (Manassas, VA, USA): MDCK-II cells; InvivoGen (San Diego, CA, USA): blasticidin, hygromycin B; Santa Cruz Biotechnology (Santa Cruz, CA, USA): goat polyclonal anti-Vangl2 antibody; Jackson Immunoresearch Laboratories (West Grove, PA, USA): Cy3-conjugated rabbit anti-goat antibody.

Expression constructs

We assembled a full-length cDNA by amplifying three over-lapping cDNA fragments from a kidney cDNA library (6)
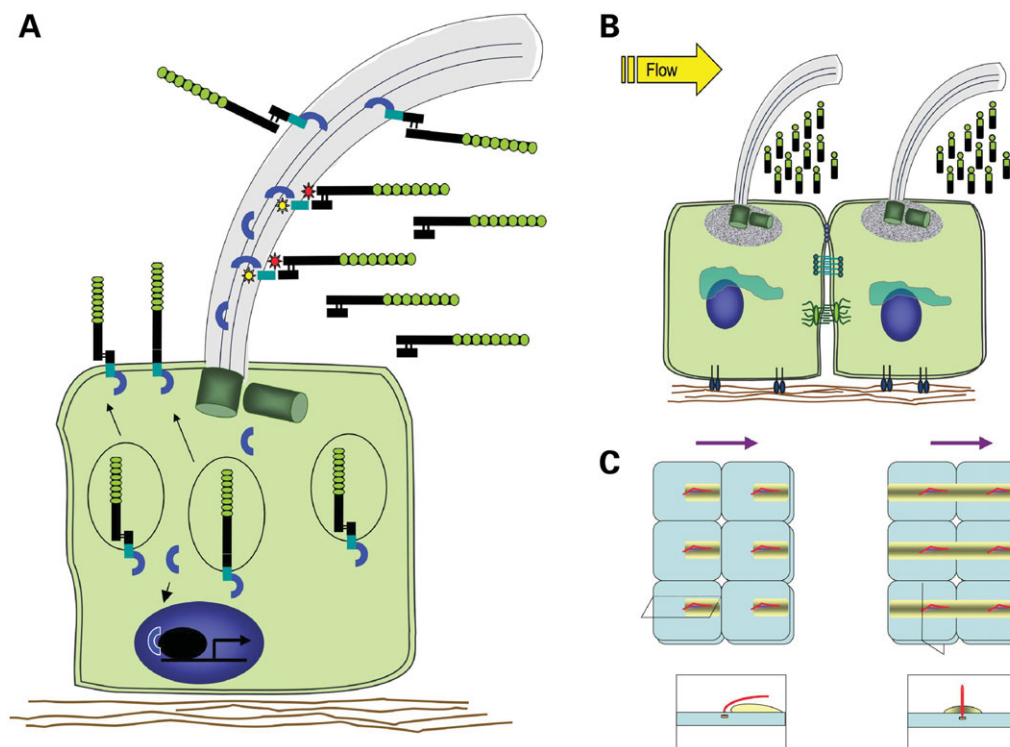
Figure 8. Model of PD1 processing and function. (**A**) A subset of PD1 molecules is subject to post-translational processing by a PC, resulting in an N-terminus that is tethered to the C-terminal product. A second set of PD1 molecules traffics to the plasma membrane without processing and undergoes constitutive release of intra-cellular cytoplasmic products. Upon metalloprotease activation, PD1 sheds its ectodomain into the lumen and the cytoplasmic C-terminus leaves the plasma membrane. (**B**) Flow-based delivery of the shed PD1 ectodomain may help maintain cellular planar orientation by helping to deliver an asymmetric gradient of signal. (**C**) Two models of how flow-based distribution of shed product could theoretically establish signal gradients and thus orientation information for tubular cells. The panels on top represent the view looking down on the cell surface of a cluster of six cells, each with a central primary cilium (red) leaning in the direction of flow (purple arrows on top). The yellow-shaded rectangle represents the signal gradient resulting from shed PD1 ectodomain. The panels on the bottom represent sections taken either along the longitudinal axis of the tubule through the primary cilium (left) or orthogonal to the direction of luminal flow through the centre of the cell (right). The two models differ in that the gradient is parallel to the direction of flow in one (left) and perpendicular to it in the other (right).

using the following sets of primers and conditions: F1: 5′-GAAAGGATCATTTCTCCCTTGAGTC-3′, R1: 5′-CA GGAACTTGACTCCATAGGGAAAG-3′; F2: 5′-GCCCAA TCAGCCAATTACCG-3′, R2: 5′-TCTTCTTAGTTGTCCCA GCAGGAC-3′ using Platinum *Taq* DNA polymerase High Fidelity (Invitrogen): 94°C for 2 min, 30 cycles of 94°C for 30 s, 64°C for 30 s, 72°C for 6 min and a final extension at 72°C for 10 min. Each product was sequenced and several point mutations were corrected by using site-directed mutagenesis. They were assembled into the largest full-length cDNA using restriction enzyme sites *Kpn*I, *Sph*I and *Bse*MI. The junctional cloning sites of the final assembled cDNA were verified by DNA sequencing. The full-length *PKHD1* cDNA was then inserted into the expression vector PCI using the restriction enzyme sites, *Xho*I and *Not*I. An expression vector with a 7×-Myc tag inserted at the C-terminus was generated by ligation using *Sal*I and *Not*I. The 6×-Myc tag DNA sequence from CS2-MT (R. Kopan, Washington University School of Medicine) was used to help construct the tag.

An expression vector with a 3×-FLAG tag or an EGFP tag inserted after the signal sequence and the adjacent two amino acids was generated by ligation using *Eco*N1 and *Sca*1 sites. An expression vector with a 3×-FLAG tag or an EGFP tag

at its N-terminus and 7×-Myc tag at its C-terminus was made by repeated ligation as described and the sequence of each junction was verified. The various *PKHD1* constructs were also cloned into the *Not*I and *Eco*RV sites of pcDNA5/FRT/TO for stable transfection.

Expression of recombinant *PKHD1* in HEK 293 and MDCK cells

For transient expression studies, pCI-*PKHD1* was transfected into HEK 293 using LipofectAMINE 2000 and analyzed for PD1 expression 24–48 h later. For studies requiring stable, inducible expression of *PKHD1*, we used the Flp-In T-Rex 293 cell line and a newly developed Flp-In T-Rex MDCK cell line (manuscript in preparation). These cell lines contain the tetracycline repressor as well as an FRT site for targeted integration. Stable cell lines were established by co-transfecting the pcDNA5/FRT/TO constructs together with the Flp recombinase expression plasmid pOG44 using LipofectAMINE 2000. Cells with proper integration of our constructs into the single FRT site of the Flp-In T-Rex 293 cells were selected in medium containing 100 μg/ml hygromycin B. After selection, cell lines were maintained in

DMEM containing 2 mM L-glutamine, 10% heat-inactivated FCS, 15 µg/ml blasticidin and 100 µg/ml hygromycin B. The Flp-In T-Rex MDCK cell lines were selected under similar conditions, except hygromycin B was at a concentration of 150 µg/ml. Stable transfectants were maintained in DMEM 10% heat-inactivated FCS, 5 µg/ml blasticidin and 150 µg/ml hygromycin B. A set of control MDCK cell lines were similarly established by transfection of empty vector (pcDNA5/FRT/TO).

Western blots and immunoprecipitation

Cells were lysed in lysis buffer (20 mM Na phosphate (pH 7.2), 150 mM NaCl, 1 mM EDTA, 10% glycerol, 1% Triton X-100 and protease inhibitor cocktail. Pervanadate was prepared just prior to use by adding sodium orthovanadate to hydrogen peroxide. The sample was subjected to electrophoresis on 3–8% gradient SDS–PAGE gels after boiling. Fractionated proteins were electrotransferred to Immobilon-P polyvinylidene difluoride membranes (Millipore, Billerica, MA, USA) and detected with monoclonal anti-Myc antibody (1:1000), polyclonal anti-FLAG antibody (1:500), 5509 anti-peptide antibody (1:1000), C2 anti-N-terminal PD1 (1:1000) antibody and 210 anti-peptide antibody (1:1000) using ECL enhanced chemiluminescence (GE Healthcare Life Science, Piscataway, NJ, USA) (16). Immunoprecipitation from cellular lysates was carried out as described previously with slight modifications (36). Cells were lysed in the buffer described earlier, and then 1 ml of total cell lysate was pre-incubated with monoclonal anti-Myc beads, polyclonal Myc beads or M2 and anti-FLAG beads at 4°C for overnight and then centrifuged at 2000g. The precipitated beads were washed extensively with cell lysis buffer and finally eluted with SDS sample buffer. The eluted supernatant was subjected to SDS–PAGE and western blot analysis.

To test for constitutive secretion of N-terminal products, *PKHD1* constructs were transfected into Flp-In T-Rex 293 cells and cultured for 24 h in the presence of serum and tetracycline, at which time the medium was replaced with serum-free medium containing 1 µg/ml tetracycline. The medium was collected 48 h later, centrifuged to remove cellular debris and then incubated with M2-beads overnight at 4°C to immunopurify the N-terminus using methods outlined above. Regulated ectodomain shedding was assayed by culturing uninduced cells of the *PKHD1*+ Flp-In T-Rex 293 stable cell line overnight in serum-free medium containing 1 µg/ml tetracycline followed by the addition of various known activators of cleavage at concentrations indicated in the text. Medium was collected at the times indicated and treated as indicated above.

Cell-surface biotinylation assay

The assay was performed using published methods (37). Stable *PKHD1*+ Flp-In T-Rex 293 cells were treated with tetracycline 1 µg/ml over night and then serum-starved for 5 h. The surface plasma membrane proteins were biotinylated by gently shaking the cells for 40 min with 3.0 mg of NHS-SS-biotin at 4°C. After biotinylation, the unreacted

biotin was scavenged by incubating the cells with the DMEM medium containing 10% FCS for 10 min. Cell lysates were subsequently prepared, centrifuged at 12 000g for 10 min and then the supernatant was incubated with streptavidin–agarose beads overnight at 4°C. The mix was subsequently centrifuged at 1000g for 5 min, with the beads washed three times prior to elution of the sample with SDS sample buffer and analysis by SDS–PAGE and western blot.

PD1 antibodies

Anti-FP2 recognizes the C-terminus of human PD1 and has been previously described (16). Anti-C2 was raised against a recombinant polypeptide derived from the extra-cellular sequence of human PD1 (amino acid 3214–3394). We generated two new rabbit polyclonal antibodies using synthetic polypeptides CPHQLMNGVSRRKVSR (5509, human PD1 amino acid 3942–3957) and WPQEPWHKVRSHHSV (210, mouse PD1 amino acid 3248–3262). The immunized rabbit serum was affinity purified using the AminoLink Plus Immobilization Kit (Pierce).

Evaluation of regulated cleavage

PD1 expression was induced in the Flp-C-terminal 7×Myc *PKHD1* HEK 293 cell line by culturing the cells overnight in serum-free medium containing tetracycline 1 µg/ml.

The Flp-C-terminal 7×-Myc *PKHD1* HEK 293 cell line was cultured overnight in serum-free medium containing a protease inhibitor (GM6001, L-685,458) and tetracycline 1 µg/ml to induce PD1 expression. The next morning, cells were treated with either calcium ionophore A23187 or PMA to stimulate cleavage, incubated for the indicated times and then harvested. Cell lysates were prepared and analyzed by immunoblotting by using anti-Myc antibody.

Confocal microscopy

Flp-C-terminal 7×-Myc *PKHD1* MDCK cells or Flp-N-terminal EGFP and C-terminal 7x-Myc MDCK cells were cultured on 12-mm Transwell filters (Corning, Acton, MA, USA) in DMEM 10% heat-inactivated FCS, 5 µg/ml blasticidin and 150 µg/ml hygromycin B. The cells were grown at least 7 days post-confluence, changing the medium every other day. The expression of PD1 was induced by addition of 1 µg/ml tetracycline 2 days before the staining. The staining was performed according to a previously described method with slight modifications (37,38). Cells were fixed in 4% paraformaldehyde in phosphate-buffered saline (PBS) for 20 min at room temperature, washed with PBS, placed in 75 mM NH$_4$Cl and 20 mM glycine in PBS at room temperature to quench the fixative and then permeabilized with −20°C methanol for 3 min. After blocking with 2% bovine serum albumin in PBS for 30 min at room temperature, the cells were incubated with primary antibodies (rabbit anti-myc antibody 1:100, mouse anti-acetylated tubulin antibody 1:400, rabbit anti-GFP antibody 1:100) overnight at 4°C. After washing, the cells were incubated with secondary antibodies (goat fluorescein-conjugated anti-rabbit IgG antibody 1:100, goat Texas Red conjugated anti-mouse IgG antibody 1:100)

for 1 h at room temperature. After washing, the cells were incubated with an Alexa-488 conjugated anti-fluorescein antibody (1:100) for 1 h at room temperature. IMCD cells were processed similarly and incubated with rabbit 5509 or C2 antibody as primary antibodies. Cells were washed in PBS before mounting in the mounting medium with DAPI (Vector). The stained cells were imaged using a Zeiss Axiovert 200 microscope with 510-Meta confocal module (Carl Zeiss, Oberkochen, Germany) using a Plan-Apochromat $100\times/1.4$ NA DIC lens with Immersol 518F oil at RT. Then, 0.2 µm Z sections were captured and 3D images were reconstructed using the AxioVision software (Carl Zeiss).

SUPPLEMENTARY MATERIAL

Supplementary Material is available at HMG Online.

ACKNOWLEDGEMENTS

REFERENCES

1. Zerres, K., Mucher, G., Becker, J., Steinkamm, C., Rudnik-Schoneborn, S., Heikkila, P., Rapola, J., Salonen, R., Germino, G.G., Onuchic, L. *et al*. (1998) Prenatal diagnosis of autosomal recessive polycystic kidney disease (ARPKD): molecular genetics, clinical experience, and fetal morphology. *Am. J. Med. Genet.*, **76**, 137–144.

2. Guay-Woodford, L.M. and Desmond, R.A. (2003) Autosomal recessive polycystic kidney disease: the clinical experience in North America. *Pediatrics*, **111**, 1072–1080.

3. Fonck, C., Chauveau, D., Gagnadoux, M.F., Pirson, Y. and Grunfeld, J.P. (2001) Autosomal recessive polycystic kidney disease in adulthood. *Nephrol. Dial. Transplant.*, **16**, 1648–1652.

4. Guay-Woodford, L. (1996) Autosomal recessive disease:clinical and genetic profiles. Watson, M.L. and Torres, V.E. (Eds), *Polycystic Kidney Disease*, Oxford University Press, Oxford, UK.

5. Zerres, K., Mucher, G., Bachner, L., Deschennes, G., Eggermann, T., Kaariainen, H., Knapp, M., Lennert, T., Misselwitz, J., von Muhlendahl, K.E. *et al*. (1994) Mapping of the gene for autosomal recessive polycystic kidney disease (ARPKD) to chromosome 6p21-cen. *Nat. Genet.*, **7**, 429–432.

6. Onuchic, L.F., Furu, L., Nagasawa, Y., Hou, X., Eggermann, T., Ren, Z., Bergmann, C., Senderek, J., Esquivel, E., Zeltner, R. *et al*. (2002) PKHD1, the polycystic kidney and hepatic disease 1 gene, encodes a novel large protein containing multiple immunoglobulin-like plexin-transcription-factor domains and parallel beta-helix 1 repeats. *Am. J. Hum. Genet.*, **70**, 1305–1317.

7. Ward, C.J., Hogan, M.C., Rossetti, S., Walker, D., Sneddon, T., Wang, X., Kubly, V., Cunningham, J.M., Bacallao, R., Ishibashi, M. *et al*. (2002) The gene mutated in autosomal recessive polycystic kidney disease encodes a large, receptor-like protein. *Nat. Genet.*, **30**, 259–269.

8. Xiong, H., Chen, Y., Yi, Y., Tsuchiya, K., Moeckel, G., Cheung, J., Liang, D., Tham, K., Xu, X., Chen, X.Z. *et al*. (2002) A novel gene encoding a TIG multiple domain protein is a positional candidate for autosomal recessive polycystic kidney disease. *Genomics*, **80**, 96–104.

9. Nagasawa, Y., Matthiesen, S., Onuchic, L.F., Hou, X., Bergmann, C., Esquivel, E., Senderek, J., Ren, Z., Zeltner, R., Furu, L. *et al*. (2002) Identification and characterization of Pkhd1, the mouse orthologue of the human ARPKD gene. *J. Am. Soc. Nephrol.*, **13**, 2246–2258.

10. Bergmann, C., Senderek, J., Windelen, E., Kupper, F., Middeldorf, I., Schneider, F., Dornia, C., Rudnik-Schoneborn, S., Konrad, M., Schmitt, C.P. *et al*. (2005) Clinical consequences of PKHD1 mutations in 164 patients with autosomal-recessive polycystic kidney disease (ARPKD). *Kidney Int.*, **67**, 829–848.

11. Sharp, A.M., Messiaen, L.M., Page, G., Antignac, C., Gubler, M.C., Onuchic, L.F., Somlo, S., Germino, G.G. and Guay-Woodford, L.M. (2005) Comprehensive genomic analysis of PKHD1 mutations in ARPKD cohorts. *J. Med. Genet.*, **42**, 336–349.

12. Furu, L., Onuchic, L.F., Gharavi, A., Hou, X., Esquivel, E.L., Nagasawa, Y., Bergmann, C., Senderek, J., Avner, E., Zerres, K. *et al*. (2003) Milder presentation of recessive polycystic kidney disease requires presence of amino acid substitution mutations. *J. Am. Soc. Nephrol.*, **14**, 2004–2014.

13. Ward, C.J., Yuan, D., Masyuk, T.V., Wang, X., Punyashthiti, R., Whelan, S., Bacallao, R., Torra, R., LaRusso, N.F., Torres, V.E. *et al*. (2003) Cellular and subcellular localization of the ARPKD protein; fibrocystin is expressed on primary cilia. *Hum. Mol. Genet.*, **12**, 2703–2710.

14. Li, J.B., Gerdes, J.M., Haycraft, C.J., Fan, Y., Teslovich, T.M., May-Simera, H., Li, H., Blacque, O.E., Li, L., Leitch, C.C. *et al*. (2004) Comparative genomics identifies a flagellar and basal body proteome that includes the BBS5 human disease gene. *Cell*, **117**, 541–552.

15. Masyuk, T.V., Huang, B.Q., Ward, C.J., Masyuk, A.I., Yuan, D., Splinter, P.L., Punyashthiti, R., Ritman, E.L., Torres, V.E., Harris, P.C. *et al*. (2003) Defects in cholangiocyte fibrocystin expression and ciliary structure in the PCK rat. *Gastroenterology*, **125**, 1303–1310.

16. Menezes, L.F., Cai, Y., Nagasawa, Y., Silva, A.M., Watkins, M.L., Da Silva, A.M., Somlo, S., Guay-Woodford, L.M., Germino, G.G. and Onuchic, L.F. (2004) Polyductin, the PKHD1 gene product, comprises isoforms expressed in plasma membrane, primary cilium, and cytoplasm. *Kidney Int.*, **66**, 1345–1355.

17. Wang, S., Luo, Y., Wilson, P.D., Witman, G.B. and Zhou, J. (2004) The autosomal recessive polycystic kidney disease protein is localized to primary cilia, with concentration in the basal body area. *J. Am. Soc. Nephrol.*, **15**, 592–602.

18. Fischer, E., Legue, E., Doyen, A., Nato, F., Nicolas, J.F., Torres, V., Yaniv, M. and Pontoglio, M. (2006) Defective planar cell polarity in polycystic kidney disease. *Nat. Genet.*, **38**, 21–23.

19. Mai, W., Chen, D., Ding, T., Kim, I., Park, S., Cho, S.Y., Chu, J.S., Liang, D., Wang, N., Wu, D. *et al*. (2005) Inhibition of Pkhd1 impairs tubulomorphogenesis of cultured IMCD cells. *Mol. Biol. Cell*, **16**, 4398–4409.

20. Duckert, P., Brunak, S. and Blom, N. (2004) Prediction of proprotein convertase cleavage sites. *Protein Eng. Des. Sel.*, **17**, 107–112.

21. Nakayama, K. (1997) Furin: a mammalian subtilisin/Kex2p-like endoprotease involved in processing of a wide variety of precursor proteins. *Biochem. J.*, **327** (Pt 3), 625–635.

22. Henrich, S., Cameron, A., Bourenkov, G.P., Kiefersauer, R., Huber, R., Lindberg, I., Bode, W. and Than, M.E. (2003) The crystal structure of the proprotein processing proteinase furin explains its stringent specificity. *Nat. Struct. Biol.*, **10**, 520–526.

23. Bergmann, C., Senderek, J., Kupper, F., Schneider, F., Dornia, C., Windelen, E., Eggermann, T., Rudnik-Schoneborn, S., Kirfel, J., Furu, L. *et al*. (2004) PKHD1 mutations in autosomal recessive polycystic kidney disease (ARPKD). *Hum. Mutat.*, **23**, 453–463.

24. Huovila, A.P., Turner, A.J., Pelto-Huikko, M., Karkkainen, I. and Ortiz, R.M. (2005) Shedding light on ADAM metalloproteinases. *Trends Biochem. Sci.*, **30**, 413–422.

25. Wilhelmsen, K. and van der Geer, P. (2004) Phorbol 12-myristate 13-acetate-induced release of the colony-stimulating factor 1 receptor cytoplasmic domain into the cytosol involves two separate cleavage events. *Mol. Cell. Biol.*, **24**, 454–464.

26. Fan, S., Hurd, T.W., Liu, C.J., Straight, S.W., Weimbs, T., Hurd, E.A., Domino, S.E. and Margolis, B. (2004) Polarity proteins control ciliogenesis via kinesin motor interactions. *Curr. Biol.*, **14**, 1451–1461.

27. Geng, L., Okuhara, D., Yu, Z., Tian, X., Cai, Y., Shibazaki, S. and Somlo, S. (2006) Polycystin-2 traffics to cilia independently of polycystin-1 by using an N-terminal RVxP motif. *J. Cell Sci.*, **119**, 1383–1395.

28. Ross, A.J., May-Simera, H., Eichers, E.R., Kai, M., Hill, J., Jagger, D.J., Leitch, C.C., Chapple, J.P., Munro, P.M., Fisher, S. *et al*. (2005)

Disruption of BardetBiedl syndrome ciliary proteins perturbs planar cell polarity in vertebrates. *Nat. Genet.*, **37**, 1135–1140.

29. De Strooper, B., Annaert, W., Cupers, P., Saftig, P., Craessaerts, K., Mumm, J.S., Schroeter, E.H., Schrijvers, V., Wolfe, M.S., Ray, W.J. *et al.* (1999) A presenilin-1-dependent gamma-secretase-like protease mediates release of Notch intracellular domain. *Nature*, **398**, 518–522.

30. Schroeter, E.H., Kisslinger, J.A. and Kopan, R. (1998) Notch-1 signalling requires ligand-induced proteolytic release of intracellular domain. *Nature*, **393**, 382–386.

31. Rauchman, M.I., Nigam, S.K., Delpire, E. and Gullans, S.R. (1993) An osmotically tolerant inner medullary collecting duct cell line from an SV40 transgenic mouse. *Am. J. Physiol.*, **265**, F416–F424.

32. Hiesberger, T., Gourley, E., Erickson, A., Koulen, P., Ward, C.J., Masyuk, T.V., Larusso, N.F., Harris, P.C. and Igarashi, P. (2006) Proteolytic cleavage and nuclear translocation of fibrocystin is regulated by intracellular Ca2+ and activation of protein kinase C. *J. Biol. Chem.*, **281**, 34357–34364.

33. Harper, J.A., Yuan, J.S., Tan, J.B., Visan, I. and Guidos, C.J. (2003) Notch signaling in development and disease. *Clin. Genet.*, **64**, 461–472.

34. Schweisguth, F. (2004) Notch signaling activity. *Curr. Biol.*, **14**, R129–R138.

35. Iwamoto, R. and Mekada, E. (2000) Heparin-binding EGF-like growth factor: a juxtacrine growth factor. *Cytokine Growth Factor Rev.*, **11**, 335–344.

36. Qian, F., Boletta, A., Bhunia, A.K., Xu, H., Liu, L., Ahrabi, A.K., Watnick, T.J., Zhou, F. and Germino, G.G. (2002) Cleavage of polycystin-1 requires the receptor for egg jelly domain and is disrupted by human autosomal-dominant polycystic kidney disease 1-associated mutations. *Proc. Natl Acad. Sci. USA*, **99**, 16981–16986.

37. Akhter, S., Cavet, M.E., Tse, C.M. and Donowitz, M. (2000) C-terminal domains of Na(+)/H(+) exchanger isoform 3 are involved in the basal and serum-stimulated membrane trafficking of the exchanger. *Biochemistry*, **39**, 1990–2000.

38. Weimbrs, T., Low, S.H., Li, X. and Kreitzer, G. (2003) SNAREs and epithelial cells. *Methods*, **30**, 191–197.